CHAPTER 36

IRON AND MANGANESE REDUCTION/OXIDATION

Martin Pentrák, Linda Pentráková, and Joseph W. Stucki
University of Illinois

INTRODUCTION

Many materials, including soils, sediments, and clay minerals, can exist in a reduced or partially reduced state, through either natural or laboratory processes. To accurately characterize such materials, they must be sampled, handled, and analyzed under conditions which prevent or minimize reoxidation. Nowhere is this phenomenon more prevalent than in wetlands. Submersion of the soil greatly impedes the diffusion of atmospheric oxygen into its pores, causing oxygen to become depleted rapidly in that environment due to microbial respiration. Once the oxygen is gone, heterotrophic microorganisms look for other electron acceptors as they continue to respire. Iron (Fe) and manganese (Mn) in constituent soil minerals, being transition metals, are readily enticed into participating in such reduction and reoxidation (redox) processes (Munch and Ottow, 1977, 1980, 1982; Munch et al., 1978; Lovley and Phillips, 1986a, b; Stucki and Getty, 1986; Lovley, 1991, 1993, 1995; Lovley et al., 1993; Genin et al., 2006; Stucki and Kostka, 2006; Dong et al., 2009; Pentráková et al., 2013) and, thus, assume the role as electron acceptors in place of oxygen. When the soil is drained or sampled, oxygen rapidly reenters the pore space and invokes reoxidation. Such redox cycles create an environment where the chemical and physical properties of the wetland soils can change dynamically over space and time with fluctuations in weather, climate, and anthropogenic activity.

In this Chapter, methods for handling and analyzing samples for the different oxidation states of Fe and Mn will be described. Sampling methods for wetlands are described in other parts of this volume and in the literature, and many are suitable for or can be adapted to exclude

atmospheric oxygen. One simple method is described here. Once a sample is acquired, specialized handling is required for its storage and preparation for analysis. Depending on the type of analysis, further adaptations of normal sample holders may also be required. Techniques and apparatus used in the author's laboratory for these purposes will be presented.

In mixed-valent or reduced Fe-bearing minerals, considerable attention is paid to the need for protecting samples from the atmosphere. Studies of Mn, on the other hand, rarely mention any such efforts. The authors suggest that failure to do so could present a serious impediment to the accurate delineation of Mn oxidation states in wetlands.

SAMPLING

A simple method for obtaining a soil sample from a wetland uses an air-tight syringe (such as an AirTite™ All-plastic Norm-Ject™ syringe, Thermo-Fisher catalog no. 14-817-35) and a rubber stopper to fit the inside of the syringe barrel. The needle end of the syringe is cut off, leaving the full diameter of the barrel exposed (Figure 1). The plunger is then inserted into the barrel and pushed in until it is flush with the exposed, cut-off end.

At the sampling site, the syringe is pushed vertically downward, cut-off end first, to the depth of the top of the sediment column to be sampled. The plunger is then held firmly in that position while the barrel is pressed deeper into the sediment, creating a suction that pulls the desired amount of sample into the barrel. The rubber stopper is then inserted into the bottom (cut-off) end of the submerged barrel. The syringe assembly with sample inside is then removed from the sampling position, the outside cleaned and dried, and the plunger and stopper taped with duct tape to prevent them from moving. This assembly is then taken to the lab for sample processing.

INERT-ATMOSPHERE SAMPLE HANDLING

Apparatus for storing and processing samples under an inert atmosphere have been described by Stucki et al. (1984, 2013) and Wu et al. (1989). Samples must be stored in an atmosphere purged with oxygen-free gas (N_2, Ar, or N_2-H_2 mixture). A variety of glove boxes are commercially available for this purpose (such as Vacuum Atmospheres, Hawthorne, California; Coy Laboratory Products, Grass Lake, Michigan). Glove bags can also be used, but are recommended only for very brief, temporary storage due to their propensity to leak and the difficulty of establishing working space within them. Glove boxes are constructed with an ante-chamber where samples can be introduced without oxygen contamination, and a regenerable oxygen scrubber through which the inside atmosphere is continuously circulated to preserve its oxygen-free condition. Other important capabilities to have inside the box are electrical power, room to place an analytical balance, bulk-head fittings through which cold-water can be circulated from the outside (for a thermo-electric cold plate used in freeze drying), a vacuum port, and shelves on which samples can be stored conveniently within reach of the gloves.

Most ante-chambers use a repetitive evacuation/inert-gas refill procedure to purge their atmospheres of oxygen. Users must recognize this and prepare their sample containers to withstand the pressure gradient between the sample vessel and the ante-chamber vacuum during this procedure. Any container with contents that will be adversely affected by exposure to vacuum must be closed with a positive seal, such as a crimp, clamp, tape, or screw cap, before being placed in the ante-chamber. For example, the plunger and rubber stopper in the syringe assembly described above will be forced out of the barrel during the ante-chamber evacuation step unless they are taped closed. Once opened inside the glove box, the atmosphere will be contaminated with the atmosphere inside the container, the extent of which depends on the

number of samples and size of container. This usually is not a large concern because the continuous purging through the oxygen scrubber will rapidly remove the contaminating oxygen.

Glove-box users must also recognize that oxygen scrubbers usually also remove H_2O, so the contents of containers left open inside the box will dehydrate. Keeping all samples inside closed containers when not in use is, therefore, highly recommended. Samples can also be freeze dried inside the glove box, using a thermo-electric cold plate as described by Stucki et al. (2013).

In order to manipulate aqueous dispersions of sediment samples, two key pieces of apparatus or their equivalent are absolutely necessary. The first is an inert-atmosphere reaction tube (IRT) (Figure 2); the second is a controlled atmosphere liquid exchanger (CALE) (Figure 3). These types of apparatus have been used for decades in the junior author's laboratory (Stucki et al., 1984), and the current versions are described in detail by Stucki et al. (2013). Briefly, the reaction vessel is a 50-mL, Oak Ridge type, polycarbonate centrifuge tube with a septum-sealed cap. Access to the sample and sample solution is accomplished by inserting 22 gauge, 6-inch, deflected-point septum-penetration needles through the septum. These reaction tubes fit well into a Sorvall centrifuge SS-34 rotor or similar, so they can be centrifuged at forces up to about 35,000 x g to separate solids from liquids.

The CALE consists of an assembly of distillation flasks containing aqueous solutions of the user's choice which can be readily deoxygenated by heating to boiling while purging with an oxygen-free gas. This apparatus is plumbed so that the supernatant in the centrifuged IRT can be removed and discarded or saved, as necessary, and replaced with a selected deoxygenated solution. This ability to exchange fluids within the sample without exposure to the atmosphere make such an apparatus invaluable for a myriad of purposes, including the determination of cation exchange capacity, cation fixation capacity, swellability, chemical composition, oxidation

state, crystal structure, specific surface area, clay-organic interactions, and any other purpose requiring control over the composition of the liquid phase in the air-sensitive sample.

Asserted efforts to exclude oxygen, as described above, are an effective, although not complete, means for retarding reoxidation. For example, Stucki et al. (2013) kept reoxidation to as little as about 10 to 15% of the initial Fe(II) content of the extreme case of fully reduced ferrugninous smectite during five centrifuge-washing steps. Without use of the CALE and IRT, more than 60% of the reduced Fe was reoxidized by the same number of washings. The reversibility of redox reactions or reoxidation also depends on other factors (Shen and Stucki, 1994; Komadel et al., 1995), such as changes in expandability of the smectite, surface hydration energy, and extent of initial reduction (Stucki et al., 2000; Ribeiro et al., 2009).

While the apparatus and procedures described above were developed for Fe-bearing systems, they should be useful for Mn-containing samples as well, although the authors have no personal experience with this. Mn is more complex than Fe due to having more oxidation states and large differences in solubilities depending on the oxidation state.

IRON

Three methods for the quantitative analysis of soils and clay minerals for Fe oxidation state were compared by Amonette et al. (1994, 1997), namely, vanadate titration (Amonette and Scott, 1991), chromophoric absorption with 1,10-phenanthroline (Komadel and Stucki, 1988; Amonette and Templeton, 1998), and Mössbauer spectroscopy. For Fe in (oxyhydr)oxides and solutions, the method by Stookey (1970) using ferrozine is often used, but this method is unreliable for silicates due to inadequate dissolution (Anastácio et al., 2008). Mössbauer

spectroscopy gives semi-quantitative Fe(II):Fe(III) ratios, but is not as well suited for quantitative analysis as are the chemical methods.

The recommended method for Fe oxidation state analysis was described by Komadel and Stucki (1988) with refinements by Amonette and Templeton (1998). This method relies on the color of the tris(1-10 phenanthroline)iron(II) complex, which has an absorbance maximum at 510 nm, for determination of Fe(II). It also relies on this complex being stable against reoxidation at low pH (Schilt, 1967), so, upon dissolution in H_2SO_4-HF solution in the presence of this chelate, the ferrous iron in the sample is immediately captured and stabilized with no further need to be protected from the atmosphere. Finally, the method relies on and takes into account the phenomenon that the reaction of ferric iron in solution with 1-10 phenanthroline is different from ferrous iron. Rather than forming tris(1,10-phenanthroline)iron(III) in solution, analogous to ferrous iron, ferric iron forms the tetrakis(l,10-phenanthroline)-μ-oxodiiron(III) complex (Wehry and Ward, 1971; David et al., 1972; Stucki, 1981), which is colorless. This dinuclear ferric complex is photochemically active and can be quantitatively reduced to tris(1,10-phenanthroline)iron(II) by exposure to light in the presence of excess 1,10-phenanthroline. The active wavelength range for this reaction is < 365 nm. Because visible light intensity extends somewhat into this region, the initial solution obtained by this method must be kept in amber bottles or under red lamps to prevent any Fe(III) initially in the sample from being photochemically reduced to ferrous iron until the Fe(II) content has been determined. This phenomenon is then exploited in the determination of total Fe (see below).

If the Fe(II) content is desired on the absolute basis of mass of sample, the best approach is to freeze dry the sample first inside the glove box (Stucki et al., 2013). A mass of about 30 mg can then be measured on the analytical balance inside the glove box, closed in the digestion

vessel, removed from the glove box, and opened to immediately receive the acid-digestion and 1,10-phenanthroline solutions. After digestion in a boiling water bath, appropriate dilutions are made and the solution is analyzed for color intensity at 510 nm. Because of the photoactivity of the tetrakis(l,10-phenanthroline)-μ-oxodiiron(III) complex, if ferric iron is also present this method has the great advantage of being able to determine total Fe (and, thus, ferric iron by difference) on the same diluted solution used to measure Fe(II), which saves duplication of all dilution steps. Subsequent to the Fe(II) analysis, complete photochemical reduction of any Fe(III) present in the sample is accomplished by exposing the sample solution to an ultraviolet light (Figure 4) where the photochemical reduction reaction occurs and is complete after about 90 min. While normal room light invokes some photochemical reduction, its wavelengths are not the optimum for achieving a quantitative conversion. Hence, the ultraviolet lamps are employed for this purpose. Absorbance values are then converted to concentration using the Beer-Lambert Law.

If a measure of only the Fe(II):total Fe ratio is desired, freeze drying is unnecessary and the sample may be submitted to the 1,10-phenanthroline method in the gel state. The concentration (*c*) ratio is obtained directly from the absorbance values (*A*) for Fe(II) and total Fe, adjusted for their absorptivities (ε) (0.1861 ± 0.0088 L/μg and 0.2015 ± 0.0029 L/μg, respectively) using the Beer-Lambert Law, viz.

$$\frac{c_{\mathrm{Fe(II)}}}{c_{\mathrm{Total\ Fe}}} = \frac{A_{\mathrm{Fe(II)}}}{A_{\mathrm{Total\ Fe}}} \cdot \frac{\epsilon_{\mathrm{Total\ Fe}}}{\epsilon_{\mathrm{Fe(II)}}} \qquad [1]$$

MANGANESE

Manganese (Mn) is a common metal in the earth's crust (~ 0.1 wt.%). It occurs in rocks and soils and is dispersed in water and air, but it is not found naturally in its pure metal state

(zero oxidation state). Manganese is a first-row transition metal (e.g. Fe, Cr, V) with similar properties and many analogous characteristics as the other metals in that row. Its properties and behavior in minerals, soils, sediments, and wetlands have been studied extensively (see, for example, Ebinger and Schulze, 1989, 1990; Rhoton et al., 1993; Schulze et al., 1995a, b; Scheinost et al., 2001; Guest et al., 2002; Li et al., 2003; Kirk, 2004; Marcus et al., 2004; Marques et al., 2004; Thompson et al., 2005, 2006; Šíma et al., 2007; Bargar et al., 2009;).

The common oxidation states of Mn in soils and sediments are II, III, and IV. Among the minerals in which it is found are birnessite (δ-MnO_2), todorokite ($(Na,Ca,K,Ba,Sr(Mn^{4+},Mn^{3+},Mg,Al)_6O_{12}\cdot 3H_2O$), manganite ($MnO(OH)$), hollandite ($(Ba(Mn^{2+}Mn^{4+})_7O_{16}$), pyrolusite ($MnO_2$), braunite ($(Mn^{2+}Mn_6^{3+}(SiO_4)O_8$), and psilomelane ($(Ba(Mn^{2+})(Mn^{4+})_8O_{16}$). In solution, its permanganate (VII) oxidation state is a strong oxidant. Mn in its II oxidation state is often found in drainage water from acid-mine (AMD) and coal-mine (CMD) drainage areas and is naturally mobile. It is carried by the drainage water into ditches, streams, and rivers, and thus reaches wetlands in ample quantities where it becomes immobilized or precipitated in its higher oxidation states (III and IV) by oxidation through active (chemically) or passive (biologically by bacteria) processes (Nealson and Ford, 1980; Chapnick et al., 1982; Greene and Madgwick, 1988; Bargar et al., 2000; Webb et al., 2005; Villalobos et al. 2006; Feng et al., 2010; Grangeon et al., 2010; Tan et al., 2010). Mn is sometimes found, but rather uncommonly, as a constituent cation in phyllosilicates.

Total Mn Analysis

Determination of total Mn requires an acid extraction/digestion step before analysis. The details vary with the specific characteristics of the sample, but treatment usually includes heating

in nitric acid, oxidation with hydrogen peroxide, and filtration and/or centrifugation to remove insoluble matter (Gambrell and Patrick, 1982). The three most widely used detection methods for total Mn in soil minerals and biological and environmental samples are (1) atomic absorption spectrophotometry (AAS) (Gauthreaux et al., 2001), (2) fluorometric analysis (Biddle and Wehry, 1978), and (3) colorimetric analysis (Beyer and Fridovich, 1988; Kostka et al., 1995). Mekonnen et al. (2013) used laser-induced breakdown spectroscopy (LIBS). This method and AAS were able to determine exchangeable Mn and Mn bound in carbonates, Mn/Fe oxides, and Mn in organic matter. Mn can also be determined by the multi-elemental methods of neutron activation analysis, plasma atomic emission, inductively coupled plasma (ICP) atomic emission spectroscopy (Pandey et al., 1998; Meneses et al., 1999; Brewer and Belzer, 2001; Chen and Ma, 2001; Espinosa et al., 2001; Llobet et al., 2002; Vaughan et al., 2012; El-Taher et al., 2013), and X-ray absorption spectroscopy (XAS) (Mackle et al., 1993; Boonfueng et al., 2005; Arai, 2011). Detection limits vary among these methods so the user should be careful to select the right one for the intended purposes (Kučera et al., 1986; Abbasi, 1988; Lavi et al., 1989; Mori et al., 1989; Zeiner et al., 2013). Llobet et al. (2002) used ICP mass spectrometry with a 0.02 mg/Kg detection limit to measure Mn in soils and plants, while Pandey et al. (1998) analyzed atmospheric particulates using ICP optical emission spectrometry with a Mn detection limit of 0.001 μg/L.

The oxidation state of Mn is closely linked to its mineralogy, so studies of the mineralogy are relevant when considering its oxidation state. Many such studies have been carried out, including using Extended X-ray absorption fine structure spectroscopy (EXAFS) (Murray et al., 1985; Friedl et al., 1997; Bargar et al., 2000; Negra et al., 2005; Cerrato et al., 2010; Tan et al., 2010). Synchrotron-based X-ray diffraction and Mn K-edge EXAFS spectroscopies have also

been used in studies such as for Mn removal from CMD. Tan et al. (2010) performed chemical (active) and biological (passive) treatments of CMD, which led to oxidative precipitation of Mn oxides (MnO_x). Also receiving significant attention is Mn in all sites of poorly crystalline hexagonal and triclinic birnessite (Lanson et al., 2000; Li et al., 2012) and in todorokite (Golden et al., 1987; Grangeon et al., 2010; Feng et al., 2010).

Mn Oxidation State Analysis

Quantitative measurement of Mn(II), Mn(III), and Mn(IV) in minerals, soils, and sediments is challenging, to say the least, and only semi-quantitative results or ratios of the various states can be expected. No consensus is yet evident as to the best method to differentiate its oxidation states, and many reports lack sufficient detail to enable replication; but, three general approaches are used: (1) direct spectroscopic analysis, (2) selective extraction, or (3) colorimetric measurement of dye complexes.

Spectroscopic Methods

Direct spectroscopic differentiation of Mn(II), Mn(III), and Mn(IV) is most easily accomplished or deduced using a synchrotron, or less quantitatively by X-ray photoelectron spectroscopy. In all such methods, however, only the ratios can be determined. Semi-quantitative amounts on a mass basis must rely on calculation from total Mn values. Knowing the Mn mineral structures is also very helpful in these determinations because a change in oxidation state of Mn also involves a change in the structure or identity of the comprising mineral.

The most commonly used spectroscopic method is X-ray absorption near-edge spectroscopy (XANES). The lines observed in the Mn K-edge XANES spectra are sensitive to

changes in oxidation state (peak position) and local coordination environment (peak shape). XANES is the principal method to determine the average oxidation state (AOS) and coordination geometry of Mn in samples maintained under natural conditions. Mn(II) has a K XANES spectrum characterized by a peak at 6553.2 eV, Mn(III) in the mineral bixbyite (Mn_2O_3) is characterized by a peak at 6557.0 eV, and Mn(IV) in birnessite is characterized by a peak at 6561.5 eV. These values often vary slightly depending on the particular mineral or phase that is present; and these minerals are never purely of the stated oxidation state but contain minor quantities of the others. Studies describing this technique have been published by Manceau et al. (1992a, b), Schulze et al. (1995), Lanson et al. (2000), Guest et al. (2002), Villalobos et al. (2003, 2006), Webb et al. (2005), Feng et al., (2010), and Grangeon et al. (2010). Chalmin et al. (2009) carried out a detailed calibration of XANES peak profiles for the full range (I to VII) of Mn oxidation states.

Other spectroscopic methods have also been used, but to a much lesser extent. The products of the heterogeneous oxidation of Mn(II)aq at the surfaces of hematite, goethite, and albite were studied by Junta et al. (1994). They used Scanning Force Microscopy (SFM), X-ray Photoelectron Spectroscopy (XPS), Scanning Electron Microscopy (SEM), Auger Electron Spectroscopy (AES), Scanning Auger Microscopy (SAM), and X-ray Diffraction (XRD). Their resulting precipitates consisted of Mn(III)-bearing oxyhydroxides, predominantly feitknechtite (β-MnOOH).

Bilinski et al. (2002) had some success using combinations of energy dispersive X-ray spectroscopy (EDS), proton induced X-ray emission spectroscopy (PIXE), X-ray diffraction (XRD), scanning electron microscopy (SEM), transmission electron microscopy (TEM),

thermogravimetry (TG), differential thermogravimetry (DTG), differential scanning calorimetry (DSC), and infrared spectroscopy (IR).

Sequential Extraction

Using sequential extraction in combination with XANES, Guest et al. (2002) established a method by which semi-quantitative assessment of Mn oxidation states in different phases within a sample can be estimated. The total Mn extracted in each step was determined by AAS and the oxidation states remaining in the solid phase were determined by XANES. Chemical and spectroscopic results were generally well correlated. The sequential extraction steps were: (1) 1 M NH_4Ac at pH 7, which extracts water-soluble and exchangeable Mn, assumed to be primarily Mn(II); (2) 1 M NH_4Ac at pH 3 to remove Mn from organic matter and microbial biomass, assumed to be primarily Mn(II); (3) 0.018 M quinol in 1 M NH_4Ac at pH 7, which is a weak reductant to dissolve readily reducible Mn (quinol is recommended over hydroxylamine hydrochloride because it is more specific for Mn and dissolves less Fe), which may be mostly Mn(III); and (IV) dithionite-citrate-bicarbonate (DCB), which is a strong reductant that reduces and solubilizes Mn in the least soluble phases, assumed to be primarily Mn(III) and Mn(IV). While this method does not give a quantitative measure of each oxidation state, it does reveal the approximate levels in the various Mn phases that are present. The oxidation state can only be inferred from the sequential extraction, but it can be determined by ratio more accurately if XANES analysis is added.

Colorimetric Dye Complexes

Colorimetric analysis can be more convenient than X-ray methods due to the more common availability of UV-Vis spectrophotometers. The underlying procedure for these methods is to extract Mn from the soil sample in the presence of an organic complex or dye (Table 1). The oxidation state is then deduced from the absorbance of the complex at the specified wavelength. The chromophoric agent may also be combined with a sequential extraction process, such as described above, to further narrow the amount and distribution of the various oxidation states within a sample. The method can be tailored to some degree, using the parameters in Table 1, to be more selective for one oxidation state or another.

SAMPLE PREPARATION FOR FURTHER ANALYSES

The methods described below were originally designed for Fe-bearing samples; but, except for Mössbauer spectroscopy, the same principles could be applied to Mn-bearing minerals if air sensitive. Individual adaptations would need to be made depending on sample characteristics.

Mössbauer Spectroscopy for Fe Analysis

Mössbauer spectroscopy (Goodman, 1980, Murad, 1988, Murad and Cashion, 2004; Stucki et al., 2007; Jaisi et al., 2008; Ribeiro et al., 2009; Bishop et al., 2010; Gorski et al., 2011) is capable of analyzing redox-active samples in either the wet or dry state, and the sample can be mounted into its holder inside the glove box in either of these states. An effective sample holder for this purpose consists of two concentric cups made of Teflon with a diameter that fits the mounting device in the spectrometer. The smaller cup fits snuggly inside the larger cup and both have a thin walled bottom (which serves as the window for the γ-ray beam). The sample is

placed in the bottom of the larger cup, then the smaller cup is inserted bottom first into the larger cup and pressed gently down to fix the sample in place. The sample thus mounted is then removed from the glove box, placed in the Mössbauer sample holder, and transferred into the safety of the inert atmosphere (either N_2 or He) of the cryostat. The smaller cup has two small holes opposite one another in its wall into which the ears of a small extraction tool can be inserted to pull the two cups apart to remove the sample after analysis.

Random orientation of the sample prevents relative intensity artifacts (Murad and Cashion, 2004). This is best accomplished by avoiding much pressure when inserting the inner cup of the sample holder. Another effective method for accomplishing this is to heat the powder to about 50 °C with benzophenone powder, which liquefies at this temperature and suspends the sample particles. Upon cooling, the sample particles are fixed in a random orientation. The dried mixture can then be ground and transferred to the sample holder. Doing all of this inside the glove box is possible, but rather tedious. A third way is to rotate the sample so it intercepts the γ-ray beam at the magic angle (54.7 °). Doing this, however, greatly decreases the cross-sectional area of the sample that is "seen" by the beam and the sample holder must be sufficiently thin to minimize the cross-sectional obstruction of the beam.

UV-Visible Spectroscopy

The presence of Fe in the crystal structure of clay minerals gives rise to a number of electronic transitions which are reflected in the UV-Visible spectrum (Banin and Lahav, 1968; Lahav and Banin, 1968; Chen et al., 1979; Sherman and Vergo, 1988; Komadel et al., 1990; Merola and Mcguire, 2009). These include an oxygen to Fe charge transfer transition (260 nm), intravalence crystal-field transitions (450 to 650 nm region) for Fe(III) in octahedral or

tetrahedral coordination, and inter-valence electron transfer transitions between Fe(II) and Fe(III) in adjacent sites (700 to 750 nm region). Reduction of the Fe produces interesting changes in these bands, but their observance requires preservation of the oxidation state during analysis. To accomplish this, the following protocols are recommended. (1) Samples may be analyzed either in suspension in transmission configuration (this can also be done using the reflectance configuration if sample settling from suspension can be taken into account), or as a powder by reflectance configuration; (2) an integrating sphere or fiber-optic probe must be used to avoid artifacts from loss of signal due to light scattering; and (3) sample holders must be designed to minimize sample exposure to oxygen in the atmosphere.

The sample should normally be loaded and sealed into an appropriate holder inside the glove box, then removed and placed in the instrument for analysis. Powdered samples reoxidize at a slower rate than liquid samples, so an absolute seal may be unnecessary in this case if the analysis can be performed within a few minutes of removing it from the glove box. An example holder is one with a circular quartz window in the front, that can be loaded from the back, then sealed by pressing an o-ring-bearing plunger into the rear opening. Liquid dispersions can be studied dynamically by circulating the fluid from the IRT through a flow-through cuvette using a peristaltic pump and tubing connected to inlet and outlet needles inserted through the septum of the IRT (Figure 5).

Some UV-Vis spectrophotometers are also equipped with near-infrared (NIR) capabilities. The powdered-sample preparations described above are also suitable for NIR analysis on such instruments.

Infrared Spectroscopy

Samples for middle- and near-infrared spectroscopic analysis (400 to 4000 cm^{-1} and 4000 to 8000 cm^{-1}, respectively) (see studies by Merola et al., 2007; Neumann et al., 2008, 2011; Bzdek and McGuire, 2009) can be prepared in much the same way as described above for UV-Vis. Powdered samples can be placed in the cup of a DRIFT accessory to obtain diffuse reflectance spectra. If a powdered mixture with KBr is desired, the sample and KBr can be mixed together inside the glove box, removed from the glove box, and packed immediately into the sample holder in the FTIR. If the instrument is continuously purged with dry N_2, the low oxygen content of the purge gas, combined with the dry sample powder, allows enough time for a spectrum to be accumulated for most purposes.

If an extended time of analysis is necessary, the sample can be prepared inside the glove box as a deposit on a ZnSe or AgCl window then transferred into an inert-atmosphere cell similar to the one described by Angell and Schaffer (1965) (Figure 6). This T-shaped glass cell (denoted the "Angell & Schaffer cell") has one leg that hangs down into the beam path and consists of two parallel walls with a circular opening near the bottom. The position of the openings corresponds with the beam path. The openings are covered by two ZnSe windows, one on each side, which are glued with a high-vacuum adhesive. The window containing the sample is stapled between two cardstock sheets that have been cut to fit the shape of the hang-down leg and with circular openings corresponding to the beam path. The sample is then placed by gravity into the beam. The valve on the ground-glass lid enables control of the atmosphere inside the cell by successive evacuation and back filling cycles with the oxygen-free gas.

Attenuated total reflectance (ATR) can also be measured on air-sensitive suspensions (Yan and Stucki, 1999, 2000) by adding a rubber gasket and flat plate seal to the top of the ATR cell (either multiple- or single-bounce types). The transfer of reduced suspension to the cell is

done using a gas-tight syringe to remove the desired amount of reduced suspension from the IRT, then expressing it onto the ATR window while flushing the window area with inert gas. The gasket and plate seal are then quickly put in place. This process minimizes the potential effects of both reoxidation and evaporation.

Preparation of KBr pellets may also be accomplished using inert-atmosphere techniques. Simply place the die and anvil from the KBr press inside the glove box, weigh the desired amounts of sample and KBr on the balance inside the glove box, mix them in an agate mortar, then transfer the proper amount into the die and insert the anvil. This assembly can be removed from the glove box long enough to press it into a pellet. It is then reinserted into the glove box through the ante-chamber. The vacuum/inert-gas refill cycles in the ante-chamber minimize exposure to atmospheric oxygen and effectively keep the pellet from rehydrating. Once inside the glove box, the die and anvil can be disassembled and the KBr pellet transferred to the Angell & Schaffer cell.

SUMMARY

The rich, redox-active environment of wetlands is responsible for many processes which are critical to environmental quality. The redox status of the constituent Fe- and Mn-bearing minerals plays an important role in these processes. Methods and apparatus to characterize the redox status of these minerals include an inert-atmosphere reaction tube (IRT) and a controlled-atmosphere liquid exchanger (CALE) which enable the exchange of liquids in air-sensitive samples while minimizing exposure to atmospheric oxygen. These capabilities enable the preparation of samples in either wet or dry states and provide control over the liquid composition. Once thus prepared, samples can be transferred to sample holders either inside a

393 glove box or with a gas-tight syringe for spectroscopic or further chemical analysis. Adequate
394 attention to the sensitivity of wetland soils to reoxidation will greatly enhance understanding of
395 the contributions of redox cycles to wetland properties.
396

REFERENCES CITED

Abbasi, S.A. 1988. Synergistic extraction and atomic absorption spectrometric determination of manganese in environmental samples using N-p-aminophenyl-2-furyl-acrylohydroxamic acid and trioctylmethyl ammonium cation. Anal. Lett. 21:1935–1944.

Adams, F. 1965. Manganese. In C.A. Black et al., editors, Methods of soil analysis. Part 2. Agron. Monogr. 9. ASA, Madison, WI. p. 1011–1018.

Adams, L.F., and W.C. Ghiorse. 1988. Oxidation state of Mn in the Mn oxide produced by Leptothrix discophora SS-1. Geochim. Cosmochim. Acta 52:2073–2076.

Amonette, J.E., and A.D. Scott. 1991. Determination of ferrous iron in non-refractory silicate minerals: 1. An improved semi-micro oxidimetric method. Chem. Geol. 92:329–338.

Amonette, J.E., and J.C. Templeton. 1998. Improvements to the quantitative assay of nonrefractory minerals for Fe(II) and total Fe using 1,10-phenanthroline. Clays Clay Miner. 46:51–62.

Amonette, J.E., F.A. Khan, H. Gan, J.W. Stucki, and A.D. Scott. 1994. Quantitative oxidation-state analysis of soils. In: Quantitative methods in soil mineralogy, SSSA miscellaneous publication. J.E. Amonette and L.W. Zelazny, editors, SSSA, Madison, WI. p. 83–113.

Amonette, J.E., F.A. Khan, H. Gan, J.W. Stucki, and A.D. Scott. 1997. Comparison of oxidimetric, spectrophotometric, and Mössbauer-spectroscopic methods for determination of Fe(II) in nonrefractory minerals. In: Proceedings Eleventh International Clay Conference, 1997. H. Kodama, A. R Mermut, and J. K. Torrance, editors. p. 277-286.

Anastácio, A.S., B. Harris, H.I. Yoo, J.D. Fabris, and J.W. Stucki. 2008. Limitations of the ferrozine method for quantitative assay of mineral systems for ferrous and total iron. Geochim. Cosmochim. Acta 72:5001–5008.

Angell, C.L., and P.C. Schaffer. 1965. Infrared spectroscopic investigations of zeolites and adsorbed molecules: I. Structural OH groups. J. Phys. Chem. 69:3463–3470.

Arai, Y. 2011. Aqueous interfacial chemistry of kaolinite for the removal of Cu(II) in the presence of birnessite: Kinetic and spectroscopic studies. Appl. Clay Sci. 53:572–580.

Banin, A., and N. Lahav. 1968. Particle size and optical properties of montmorillonite in suspension. Isr. J. Chem. 6:235–250.

Bargar, J.R., B.M. Tebo, and J.E. Villinski. 2000. In situ characterization of Mn(II) oxidation by spores of the marine Bacillus sp. strain SG-1. Geochim. Cosmochim. Acta 64:2775–2778.

Bargar, J.R., C.C. Fuller, M.A. Marcus, A.J. Brearley, M.P. De la Rosa, S.M. Webb, and W.A. Caldwell. 2009. Structural characterization of terrestrial microbial Mn oxides from Pinal Creek, AZ. Geochim. Cosmochim. Acta 73:889–910.

Beyer, Jr., W.F., and I. Fridovich. 1988. An ultrasensitive colorimetric assay for manganese. Anal. Biochem. 170:512–519.

Biddle, V.L., and E.L. Wehry. 1978. Fluorometric determination of manganese(II) via catalyzed enzymatic oxidation of 2,3-diketogulonate. Anal. Chem. 50:867–870.

Bilinski, H., R. Giovanoli, A. Usui, and D. Hanžel. 2002. Characterization of Mn oxides in cemented streambed crusts from Pinal Creek, Arizona U.S.A., and in hot-spring deposits from Yuno-Taki Falls, Hokkaido, Japan. Am. Min. 87:580–591.

441 Bishop, M.E., D.P. Jaisi, H. Dong, R.K. Kukkadapu, and J. Ji. 2010. Bioavailability of Fe(III) in
442 loess sediments: An important source of electron acceptors. Clays Clay Miner. **58:**542-
443 557.
444 Boonfueng, T., L. Axe, and Y. Xu. 2005. Properties and structure of manganese oxide-coated
445 clay. J. Colloid Interf. Sci. 281:80–92.
446 Brewer, R., and W. Belzer. 2001. Assessment of metal concentrations in atmospheric particles
447 from Burnaby Lake, British Columbia, Canada. Atmos. Environ. 35:5223–5233.
448 Bromfield, S.M. 1958. The properties of a biologically formed manganese oxide, its availability
449 to oats and its solution by root washings. Plant Soil 9:325–337.
450 Bzdek, B.R., and M.M. McGuire. 2009. Polarized ATR-FTIR investigation of Fe reduction in
451 the Uley nontronites. Clays Clay Miner. **57:**227-233.
452 Cerrato, J.M., M.F., Hochella, Jr., W.R. Knocke, A.M. Dietrich, and T.F. Cromer. 2010. Use of
453 XPS to identify the oxidation state of Mn in solid surfaces of filtration media oxide
454 samples from drinking water treatment plants. Environ. Sci. Technol. 44:5881–5886.
455 Chalmin, E., F. Farges and G.E. Brown. 2009. A pre-edge analysis of Mn K-edge XANES
456 spectra to help determine the speciation of manganese in minerals and glasses. Contrib.
457 Mineral. Petrol. 157:111–126.
458 Chapnick, S.D., W.S. Moore, and K.H. Nealson. 1982. Microbially mediated manganese
459 oxidation in a freshwater lake. Limnol. Oceanogr. 27:1004–1014.
460 Chen, Y., D. Shaked, and A. Banin. 1979. The role of structural iron(III)in the UV absorpiton by
461 smectites. Clay Miner. 14:93–102.
462 Chen, M., and L.Q. Ma. 2001. Comparison of three aqua regia digestion methods for twenty
463 Florida soils. Soil Sci.Soc. Am. J. 65:491–499.

D’Amore, D.V., S.R. Stewart, and J.H. Huddleston. 2004. Saturation, reduction, and the formation of iron–manganese concretions in the Jackson-Frazier wetland, Oregon. Soil Soil Sci.Soc. Am. J. 68:1012–1022.

David, P.G., J.G. Richardson, and E.L. Wehry. 1972. Photore- duction of tetrakis(1,10-phenanthroline)-mu-oxodiiron(III) complexes in aqueous and acetonitrile solution. J. Inorg. Nucl. Chem. 34:1333–1346.

Delfino, J.J., and G.F. Lee. 1968. Chemistry of manganese in lake Mendota, Environ. Sci. Technol. 2:1094–1100.

Dong, H., D.P. Jaisi, J. Kim, and G. Zhang. 2009. Microbe-clay mineral interactions. Am. Min. 94:1505–1519.

Ebinger, M.H., and D.G. Schulze. 1989. Mn-substituted goethite and Fe-substituted groutite synthesized at acid pH. Clays Clay Miner. 37:151–156.

Ebinger, M.H., and D.G. Schulze. 1990. The influence of pH on the synthesis of mixed Fe-Mn oxide minerals. Clay Miner. 25:507–518.

El-Taher, A., A.A. Ibraheem, and S. Abdelkawy. 2013. Elemental analysis of marble used in Saudi Arabia by different nuclear analytical techniques. Appl. Radiat. Isot. 73:17–20.

Espinosa, A.J.F., M. Ternero-Rodriguez, F.J. Barragan de la Rosa, and J.C. Jimenez-Sanchez. 2001. Size distribution of metals in urban aerosols in Seville (Spain). Atmos. Environ. 35:2595–2601.

Feng, X.H., M. Zhu, M. Ginder-Vogel, C. Ni, S.J. Parikh, and D.L. Sparks. 2010. Formation of nano-crystalline todorokite from biogenic Mn oxides. Geochim. Cosmochim. Acta 74:3232–3245.

Friedl, G., B. Wehrli, and A. Manceau. 1997. Solid phases in the cycling of manganese in eutrophic lakes: New insights from EXAFS spectroscopy. Geochim. Cosmochim. Acta 61:275–290.

Gambrell, R.P., and W.H. Patrick, Jr. 1982. Manganese. In: A.L. Page, R.H. Miller and D.R. Keeney, editors, Methods of soil analysis. Part 2. 2nd ed. Agron. Monogr. 9. ASA and SSSA, Madison, WI. p. 313–322.

Gauthreaux, K., C. Hardaway, T. Falgoust, C.O. Noble, J. Sneddon, M.J. Beck, and J.N. Beck. 2001. Manganese species migration in soil at the Sabine National Wildlife Refuge, Louisiana. J. Environ. Monit. 3:487–492.

Genin, J.M.R., M. Abdelmoula, C. Ruby, and C. Upadhyay. 2006. Speciation of iron; characterisation and structure of green rusts and Fe(II)-(III) oxyhydroxycarbonate fougerite. C.R. Geosci. 338:402–419.

Ghiorse, W.C. 1984. Bacterial Transformations of manganese in wetland environments. In: C.A. Reddy and King, M.J., editors, Current Perspectives in Microbial Ecology. American Society of Microbiology, Washington D.C., p. 615–622.

Golden, D.C., C.C. Chen, and J.B. Dixon. 1987. Transformation of birnessite to buserite, todorokite, and manganite under mild hydrothermal treatment. Clays Clay Miner. 35:271–280.

Goodman, B.A. 1980. Mössbauer spectroscopy. In: J.W. Stucki and W.L. Banwart, editors, Advanced Chemical Methods in Soil and Clay Mineral Research. Reidel, Dordrecht, Boston. p. 1–92.

Gorski, C.A., A. Neumann, M. Sander, and T.B. Hofstetter. 2011. Assessing the redox properties of structural iron-bearing clay minerals using electrochemical and spectroscopic approaches. Abstracts of Papers of the American Chemical Society **242:**

Grangeon, S., B. Lanson, N. Miyata, Y. Tani, and A. Manceau. 2010. Structure of nanocrystalline phyllomanganates produced by freshwater fungi. Am. Min. 95:1608–1616.

Greene, A.C., and J.C. Madgwick. 1988. Heterotrophic manganese-oxidizing bacteria from Groote Eylandt, Australia. Geomicrobiol. J. 6:119–127.

Grill, E.V. 1982. Kinetic and thermodynamic factors controlling manganese concentrations in oceanic waters. Geochem. Cosmochim. Acta 46:2435–2446.

Guest, C.A., D.G. Schulze, I.A. Thompson, and D.M. Huber. 2002. Correlating manganese X-ray absorption near-edge structure spectra with extractable soil manganese. Soil Sci. Soc. Am. J. 66:1172–1181.

Hallberg, K.B., and D.B. Johnson. 2005. Biological manganese removal from acid mine drainage in constructed wetlands and prototype bioreactors. Sci. Total Environ. 338:115–124.

Hem, J.D., 1981. Rates of manganese oxidation in aqueous systems. Geochim. Cosmochim. Acta 45:1369–1374.

Hem, J.D., and C.J. Lind. 1983. Nonequilibrium models for predicting forms of precipitated manganese oxides. Geochim. Cosmochim. Acta 41:2037–2046.

Jaisi, D.P., H. Dong, and J.P. Morton. 2008. Partitioning of Fe(II) in reduced nontronite (NAu-2) to reactive sites: Reactivity in terms of Tc(VII) reduction. Clays Clay Miner. **56:**175-189.

Johnson, D., and B.Chiswell. 1993. A new method for the evaluation of the oxidizing equivalent of manganese in surface freshwaters. Talanta 40:533–540.

530 Junta, J.L., and M.F. Hochella, Jr. 1994. Manganese (II) oxidation at mineral surfaces: A
531 microscopic and spectroscopic study. Geochim. Cosmochim. Acta 58:4985–4999.
532 Kessick, M.A., and J.J. Morgan. 1975. Mechanism of autoxidation of manganese in aqueous
533 solution. Environ. Sci. Technol. 9:157–159.
534 Kirk, G. 2004. The biogeochemistry of submerged soils. John Wiley & Sons, Chicester, UK. p.
535 290.
536 Komadel, P., and J.W. Stucki. 1988. Quantitative assay of minerals for Fe^{2+} and Fe^{3+} using 1,10-
537 phenanthroline: III. A rapid photochemical method. Clays Clay Miner. 36:379–381.
538 Komadel, P., P.R. Lear, and J.W. Stucki. 1990. Reduction and reoxidation of nontronite - extent
539 of reduction and reaction-rates. Clays Clay Miner. 38:203–208.
540 Komadel, P., J. Madejová, and J.W. Stucki.1995. Reduction and reoxidation of nontronite -
541 questions of reversibility. Clays Clay Miner. 43:105–110.
542 Kostka, J., G.W. Luther, and K.H. Nealson. 1995. Chemical and biological reduction of Mn (III)
543 -pyrophosphate complexes: Potential importance of dissolved Mn (III) as an
544 environmental oxidant. Geochim. Cosmochim. Acta 59:885–894.
545 Kučera, J., L. Soukal, and J. Faltejsek. 1986. Low level determination of manganese in biological
546 reference materials by neutron activation analysis. J. Radioanal. Nucl. Chem. 107:361–
547 369.
548 Lahav, N., and A. Banin. 1968. Effect of various treatments on particle size and optical
549 properties of montmorillonite suspensions. Isr. J. Chem. 6:285–294.
550 Lanson, B., V.A. Drits, E. Silvester, and A. Manceau. 2000. Structure of H-exchanged hexagonal
551 birnessite and its mechanism of formation from Na-rich monoclinic buserite at low pH.
552 Am. Min. 85:826–838.

553 Lavi, N., F. Lux, and Z.B. Al-Fassi. 1989. Determination of magnesium, aluminum, phosphorus,
554 copper and manganese in biological fluids by neutron activation analysis. J. Radioanal.
555 Nucl. Chem. 129:93–102.
556 Li, C., B. Zhang, T. Ertunc, A. Schaeffer, and R. Ji. 2012. Birnessite-induced binding of
557 phenolic monomers to soil humic substances and nature of the bound residues. Environ.
558 Sci. Technol. 46:8843–8850.
559 Li, H., L.S. Lee, D.G. Schulze, and C.A. Guest. 2003. Role of soil manganese in the oxidation of
560 aromatic amines. Environ. Sci. Technol. 37:2686–2693.
561 Llobet, J.M., M. Schuhmacher, and J.L. Domingo. 2002. Spatial distribution and temporal
562 variation of metals in the vicinity of a municipal solid waste incinerator after a
563 modernization of the flue gas cleaning systems of the facility. Sci. Total Environ.
564 284:205–214.
565 Lovley, D.R. 1991. Dissimilatory Fe(III) and Mn(IV) reduction. Microbiol. Rev. 55:259–287.
566 Lovley, D.R. 1993. Dissimilatory metal reduction. Annu. Rev. Microbiol. 47:263–290.
567 Lovley, D.R. 1995. Microbial reduction of iron, manganese, and other metals. Adv. Agron.
568 54:175–231.
569 Lovley, D.R., and E.J.P. Phillips. 1986a. Organic-matter mineralization with reduction of ferric
570 iron in anaerobic sediments. Appl. Environ. Microbiol. 51, 683–689.
571 Lovley, D.R., and E.J.P. Phillips. 1986b. Availability of ferric iron for microbial reduction in
572 bottom sediments of the fresh-water tidal potomac river. Appl. Environ. Microbiol.
573 52:751–757.
574 Lovley, D.R., S.J. Giovannoni,.D.C. White, J.E. Champine, E.J.P. Phillips, Y.A. Gorby, and S.
575 Goodwin. 1993. Geobacter-metallireducens gen-nov sp-nov, a microorganism capable of

coupling the complete oxidation of organic-compounds to the reduction of iron and other metals. Arch. Microbiol. 159:336–344.

Mackle, P., J.M. Charnock, and C.D. Garner. 1993. Characterization of the manganese core of reconstituted ferritin by X-ray absorption spectroscopy, J. Am. Chem. Soc. 115:8471–8472.

Manceau, A., A.I. Gorshkov, and V.A. Drits. 1992a. Structural chemistry of Mn, Fe, Co, and Ni in manganese hydrous oxides: I. Information from XANES spectroscopy. Am. Min. 77:1133–1143.

Manceau, A., A.I. Gorshkov, and V.A. Drits. 1992b. Structural chemistry of Mn, Fe, Co, and Ni in manganese hydrous oxides: II. Information from EXAFS spectroscopy and electron and X-ray-diffraction. Am. Min. 77:1144–1157.

Marcus, M.A., A. Manceau, and M. Kersten. 2004. Mn, Fe, Zn and As speciation in a fast-growing ferromanganese marine nodule. Geochim. Cosmochim. Acta 68:3125–3136.

Marques, J.J., D.G. Schulze, N. Curi, and S.A. Mertzman. 2004. Trace element geochemistry in Brazilian Cerrado soils. Geoderma 121:31–43.

Mekonnen, K.N., A.A. Ambushe, B.S. Chandravanshi, M.R. Abshiro, A. du Plessis, and R.I. McCrindle. 2013. Assessment of the concentration of Cr, Mn and Fe in sediment using laser-induced breakdown spectroscopy. B. Chem. Soc. Ethiopia. 27:1–13.

Meneses, M., J.M. Llobet, S. Granero, M. Schuhmacher, and J.L. Domingo. 1999. Monitoring metals in the vicinity of a municipal waste incinerator: Temporal variation in soils and vegetation. Sci. Total Environ. 226:157–164.

Merola, R.B., and M.M. McGuire. 2009. Crystallographic site distribution and redox activity of Fe in nontronites determined by optical spectroscopy. Clays Clay Miner. 57:771–778.

599 Merola, R. B., E. D. Fournier, and M. M. McGuire. 2007. Spectroscopic investigations of Fe^{2+}
600 complexation on nontronite clay. Langmuir **23:**1223-1226.
601 Morgan, J.J., and W. Stumm. 1965. Analytical chemistry of aqueous manganese. J. Am. Water
602 Works Assoc. 57:107–119.
603 Mori, I., Y. Fujita, K. Ikuta, Y. Nakahashi, and K. Kato. 1989. Highly sensitive and selective
604 fluorimetric methods for the determination of iron (III) and manganese (II) using
605 fluorescein–hydrogen peroxide–triethylenetetramine and fluorescein–hydrogen peroxide–
606 triethylenetetramine/iron, respectively. Fresenius Z. Anal. Chem. 334:252–255.
607 Munch, J.C., and J.C.G. Ottow. 1977. Model experiments on the mechanism of bacterial iron-
608 reduction in water-logged soils. Z. Pflanzenernähr. Bodenk. 140:549–562.
609 Munch, J.C., and J.C.G. Ottow. 1980. Preferential reduction of amorphous to crystalline iron
610 oxides by bacterial activity. Soil Sci. 129:15–21.
611 Munch, J.C., and J.C.G. Ottow. 1982. Effect of cell contact iron(III)-oxide form on bacterial iron
612 reduction. Z. Pflanzenernähr. Bodenk. 145:66–77.
613 Munch, J.C., T. Hillebrand, and J.C.G. Ottow. 1978. Transformation in the Fe_o/Fe_d ratio of
614 pedogenic iron oxides affected by iron-reducing bacteria. Can. J. Soil Sci. 58:475–486.
615 Murad, E. 1988. Properties and behavior of iron oxides as determined by Mössbauer
616 spectroscopy. In: J.W. Stucki, B.A. Goodman, and U. Schwertmann, editors, Iron in soils
617 and clay minerals. D. Reidel, Dordrecht, The Netherlands. p. 309–350.
618 Murad, E., and J.D. Cashion. 2004. Mössbauer spectroscopy of environmental materials and
619 their industrial utilization. Kluwer, Boston.
620 Murray, J.W., L.S. Balistrieri, and B. Paul. 1984. The oxidation state of manganese in marine
621 sediments and ferromanganese nodules. Geochim. Cosmochim. Acta 48:1237–1247.

622 Murray, J.W., J.G. Dillard, R. Giovanoli, H. Moers, and W. Stumm. 1985. Oxidation of Mn(II):
623 Initial mineralogy, oxidation state and ageing. Geochim. Cosmochim. Acta 49:463–470.
624 Nealson, K.H., and J. Ford. 1980. Surface enhancement of bacterial manganese oxidation:
625 implications for aquatic environments. Geomicrobiol. J. 2:21–37.
626 Negra, C., D.S. Ross, and A. Lanzirotti. 2005. Oxidizing behavior of soil manganese:
627 Interactions among abundance, oxidation state, and pH. Soil Sci.Soc. Am. J. 69:87–95.
628 Neumann, A., T.B. Hofstetter, M. Lüssi, O.A. Cirpka, S. Petit, and R.P. Schwarzenbach. 2008.
629 Assessing the redox reactivity of structural iron in smectites using nitroaromatic
630 compounds as kinetic probes. Environ. Sci. Technol. **42:**8381-8387.
631 Neumann, A., S. Petit, and T.B. Hofstetter. 2011. Evaluation of redox-active iron sites in
632 smectites using middle and near infrared spectroscopy. Geochim. Cosmochim. Acta
633 **75:**2336-2355.
634 Ormerod, J.G. 1966. A simple method for the detection of oxidized manganese in particles on
635 membrane filters. Limnol. Oceanogr. 11:635–636.
636 Pandey, P.K., K.S. Patel, and P. Subrt. 1998. Trace elemental composition of atmospheric
637 particulate at Bhilai in central-east India. Sci. Total Environ. 215:123–134.
638 Pentráková, L., K. Su, M. Pentrák, and J.W. Stucki. 2013. A review of microbial redox
639 interactions with structural Fe in clay minerals. Clay Miner. 48: In Review
640 Piper, D.Z., J.R. Basler, and J.L. Bischoff. 1984. Oxidation state of manganese nodules.
641 Geochim. Cosmochim. Acta 48:2347–2355.
642 Rhoton, F.E., J.M. Bigham, and D.G. Schulze. 1993. Properties of iron-manganese nodules from
643 a sequence of eroded fragipan soils. Soil Sci.Soc. Am. J. 57:1386–1392.

644 Ribeiro, F.R., J.D. Fabris, J.E. Kostka, P. Komadel, and J.W. Stucki. 2009. Comparisons of
645 structural iron reduction in smectites by bacteria and dithionite: I. A variable-temperature
646 Mössbauer spectroscopic study of garfield nontronite. Pure Appl. Chem. 81:1499–1509.
647 Scheinost, A.C., H. Stanjek, D.G. Schulze, U. Gasser and D.L. Sparks. 2001. Structural
648 environment and oxidation state of Mn in goethite-groutite solid-solutions. Am. Min.
649 86:139–146.
650 Schilt, A.A. 1967. Analytical applications of 1,10-phenanthroline and related compounds.
651 Pergamon 1–101.
652 Schulze, D.G., T. McCaybuis, S.R. Sutton, and D.M. Huber. 1995a. Manganese oxidation-states
653 in gaeumannomyces-infested wheat rhizospheres probed by micro-XANES spectroscopy.
654 Phytopathology 85:990–994.
655 Schulze, D.G., S.R. Sutton, and S. Bajt. 1995b. Determining manganese oxidation state in soils
656 using X-ray absorption near-edge structure (XANES) spectroscopy. Soil Sci. Soc. Am. J.
657 59:1540–1548.
658 Shen, S., and J.W. Stucki. 1994. Effects of iron oxidation state on the fate and behavior of
659 potassium in soils. In: J.L. Havlin and J. Jacobsen, editors, Soil testing: Prospects for
660 improving nutrient recommendations. SSSA, Madison, WI. p. 173–185.
661 Sherman, D.M., and N.Vergo.1988. Optical (diffuse reflectance) and Mössbauer spectroscopic
662 study of nontronite and related Fe-bearing smectites. Am. Min. 73:1346–1354.
663 Stookey, L.L. 1970. Ferrozine – a new spectrophotometric reagent for iron. Anal. Chem. 42:79–
664 81.
665 Stucki, J.W. 1981. The quantitative assay of minerals for Fe^{2+} and Fe^{3+} using 1,10-
666 phenanthroline: II. A photochemical method. Soil Sci.Soc. Am. J. 45:638–641.

667 Stucki, J.W., and J.P. Getty. 1986. Microbial reduction of iron in nontronite. Agronomy
668 Abstracts. p. 279.
669 Stucki, J.W., and J.E. Kostka. 2006. Microbial reduction of iron in smectite. C.R. Geosci.
670 338:468–475.
671 Stucki, J.W., D.C. Golden, and C.B. Roth. 1984. Preparation and handling of dithionite-reduced
672 smectite suspensions. Clays Clay Miner. 32:191–197.
673 Stucki, J.W., K. Lee, B.A. Goodman, and J.E. Kostka. 2007. Effects of in situ biostimulation on
674 iron mineral speciation in a sub-surface soil. Geochim. Cosmochim. Acta **71:**835-843.
675 Stucki, J.W., M. Pentrák, K. Su and L. Pentráková. 2013. Controlled atmosphere methods for
676 redox-activated smectites. Clay Miner. 48: (Submitted)
677 Stucki, J.W., J. Wu, H. Gan, P. Komadel, and A. Banin. 2000. Effects of iron oxidation state and
678 organic cations on dioctahedral smectite hydration. Clays Clay Miner. 48:290–298.
679 Šíma, J., K. Diáková, and V. Holcová. 2007. Redox processes of sulfur and manganese in a
680 constructed wetland. Chem. Biodiversity 4:2900–2912.
681 Tan, H., G. Zhang, P.J. Heaney, S.M. Webb, and W.D. Burgos. 2010. Characterization of
682 manganese oxide precipitates from Appalachian coal mine drainage treatment systems.
683 Appl. Geochem. 25:389–399.
684 Thompson, I.A., D.M. Huber, C.A. Guest and D.G. Schulze. 2005. Fungal manganese oxidation
685 in a reduced soil. Environ. Microbiol. 7:1480–1487.
686 Thompson, I.A., D.M. Huber, and D.G. Schulze. 2006. Evidence of a multicopper oxidase in Mn
687 oxidation by Gaeumannomyces graminis var. tritici. Phytopathology 96:130–136.
688 Tipping, E. 1984. Temperature dependence of Mn(II) oxidation in lakewaters: A test of
689 biological involvement. Geochim. Cosmochim. Acta 48:1353–1356.

690 Tipping, E., D.W. Thompson, and J.H. Davison. 1984. Oxidation products of Mn(II) in lake
691 waters. Chem. Geol. 44:359–383.
692 Vaughan, P.P., M.P. Bruns, C.L. Beck, and M. Cochran. 2012. Removal efficiency of heavy
693 metals using various resins and natural materials. J. App. Sci. 12:2065–2070.
694 Villalobos, M., B. Toner, J. Bargar, and G. Sposito. 2003. Characterization of the manganese
695 oxide produced by Pseudomonas putida strain MnB1. Geochim. Cosmochim. Acta
696 67:2649–2662.
697 Villalobos, M., B. Lanson, A. Manceau, B. Toner, and G. Sposito. 2006. Structural model for the
698 biogenic Mn oxide produced by Pseudomonas putida. Am. Min. 91:489–502.
699 Webb, S.M., B.M. Tebo, and J.R. Bargar. 2005. Structural characterization of biogenic
700 manganese oxides produced in seawater by the marine Bacillus sp. strain SG-1. Am. Min.
701 90:1342–1357.
702 Wehry, E.L., and R.A.Ward. 1971. Photoreduction of tris(1,10-phenanthroline)iron(III). Inorg.
703 Chem. 10:2660–2664.
704 Wu, Y., and B. Deng. 2006. Inhibition of FeS on chromium(III) oxidation by biogenic
705 manganese oxides. Environ. Eng. Sci. 23:552-560.
706 Wu, J., P.F. Low, and C.B. Roth. 1989. Effects of octahedral-iron reduction and swelling
707 pressure on interlayer distances in na-nontronite. Clays Clay Miner. 37:211–218.
708 Yan, L., and J.W. Stucki. 1999. Effects of structural fe oxidation state on the coupling of
709 interlayer water and structural Si-O stretching vibrations in montmorillonite. Langmuir
710 15:4648–4657.
711 Yan, L.B., and J.W. Stucki. 2000. Structural perturbations in the solid-water interface of redox
712 transformed nontronite. J. Colloid Interf. Sci. 225:429–439.

713 Zeiner, M., I.J. Cindrić, I.L. Mikelić, G. Medunić, Š. Kampić, N. Tomašić, and G. Stingeder.
714 2013. The determination of the extractability of selected elements from agricultural soil.
715 Environ. Monit. Assess. 185:223–229.
716

FIGURE CAPTIONS

Figure 1. Illustration of cut-off syringe for use in sampling of saturated sediments in a wetland.

Figure 2. Illustration of the design of an inert-atmosphere reaction tube (IRT) (used with permission from Stucki et al., 2013))

Figure 3. Photo of a controlled atmosphere liquid exchanger (CALE). For a more detailed illustration, see Stucki et al. (2013).

Figure 4. Photo of ultra-violet light box used to photochemically reduce tetrakis(l,10-phenanthroline)-μ-oxodiiron(III) to tris(1,10-phenanthroline)iron(II) in order to obtain total Fe in a sample.

Figure 5. Illustration of the circuit used to obtain UV-Vis spectra of aqueous dispersions of reduced clay minerals (used with permission fom Stucki et al., 2013).

Figure 6. Photo of a glass vacuum cell used to obtain infrared spectra of air-sensitive samples (patterned after Angell and Schaffer, 1965).

731

732 Table 1. Summary of organic complexes or dyes that form with the various oxidation states of

733 Mn, along with the wavelength (λ) of maximum absorbance.

734

Complex or Dye	Oxidation State	λ (nm)	Reference
Pyrophosphate	Mn(III)	480	Kostka et al. (1995)
T-(4-CP)P porphyn	Mn(II)	468	Johnson and Chiswell (1993)
Leuco Crystal Violet (LCV)*	Mn(III)	590	Johnson and Chiswell (1993)
Leuco Crystal Violet (LCV)*	Mn(IV)	590	Johnson and Chiswell (1993); Delfino and Lee (1968); Murray et al. (1984); Ghiorse (1984),
o-Tolidine	Mn(IV) Mn(II)	440	Johnson and Chiswell (1993) Murray et al. (1984) Kessick and Morgan (1975) Tipping et al. (1984)
N,N-diethyl-p-phenylenediamine (DPD)	Mn(IV)	552	Johnson and Chiswell (1993)
formaldoxime	Mn(II)	450	Hallberg and Johnson (2005)
1,10 - phenanthroline	Mn(II)	510	D'Amore et al. (2004)
Iodate	Mn(II)	540	Adams (1965); Murray et al. (1984); Adams and Ghiorse (1988)
Oxalate (reducing agent)	Mn(IV) to Mn(II)	Excess of oxalate determined by MnO_4^-	Bromfield (1958); Hem and Lind (1983); Hem (1981); Grill (1982); Piper et al. (1984)
Leuco Berbelin Blue	Mn(II)	620	Wu and Deng (2006)
Benzidine	Mn(II)	spot test	Nealson and Ford (1980); Chapnick et al. (1982); Greene and Madgwick (1988)
Leuco Malachite Green	Mn(II)	615	Morgan and Stumm (1965); Ormerod (1966)

735 *With time, the absorbance for Mn(IV) becomes greater than for Mn(III).

736

737 Figure 1

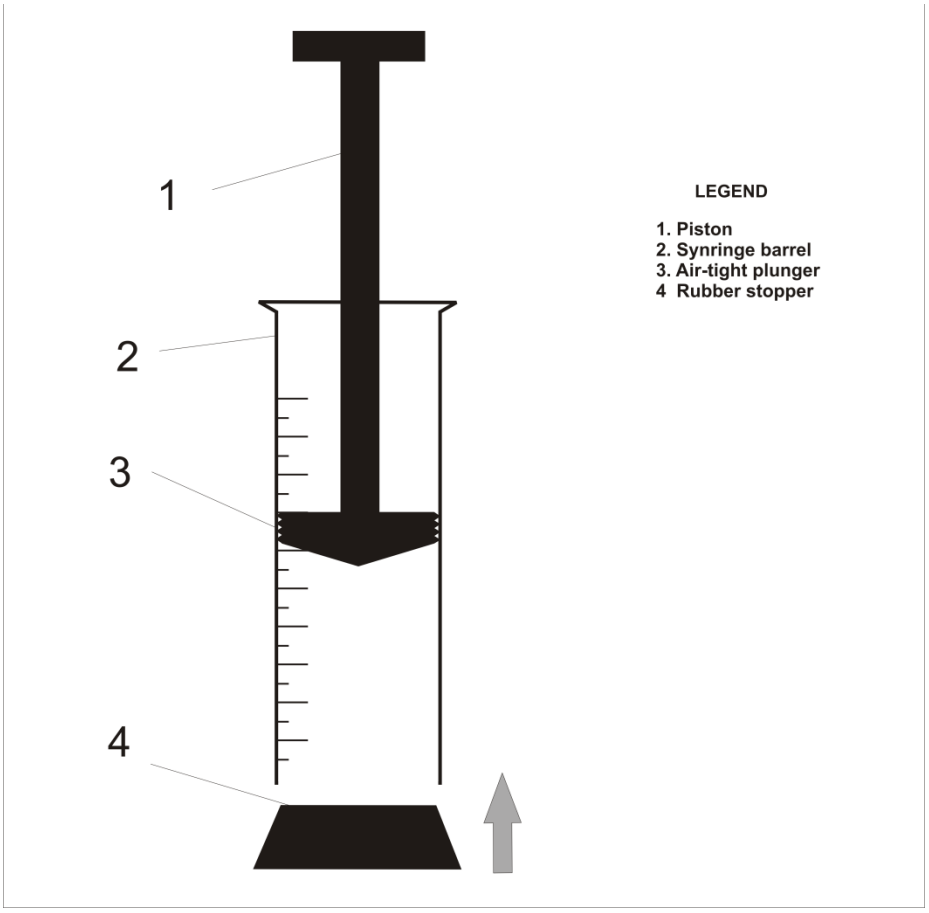

738

739

740 Figure 2

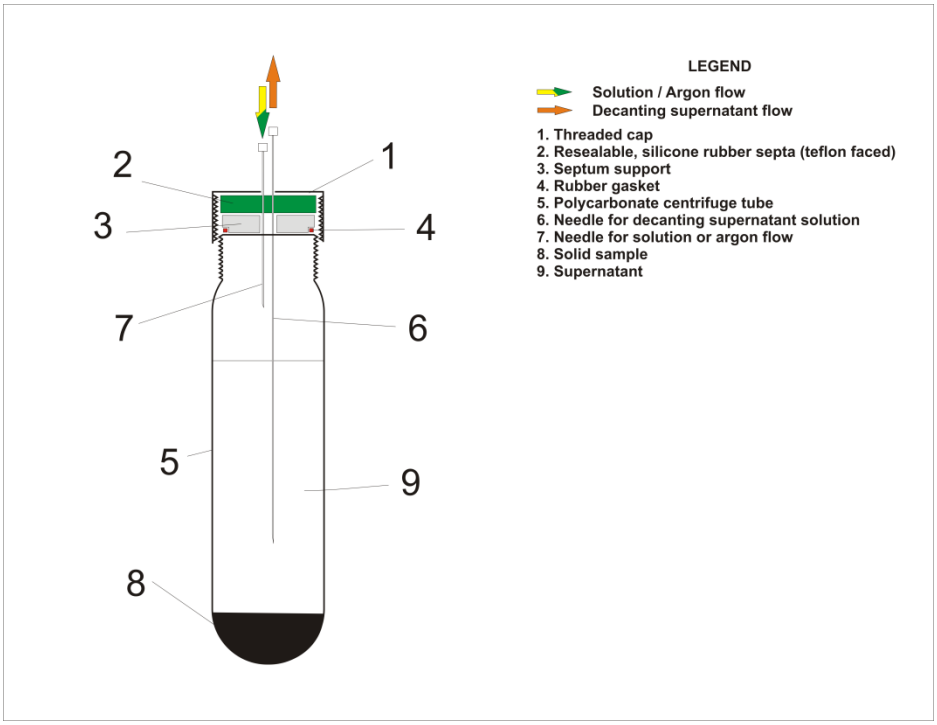

741

742

743 Figure 3

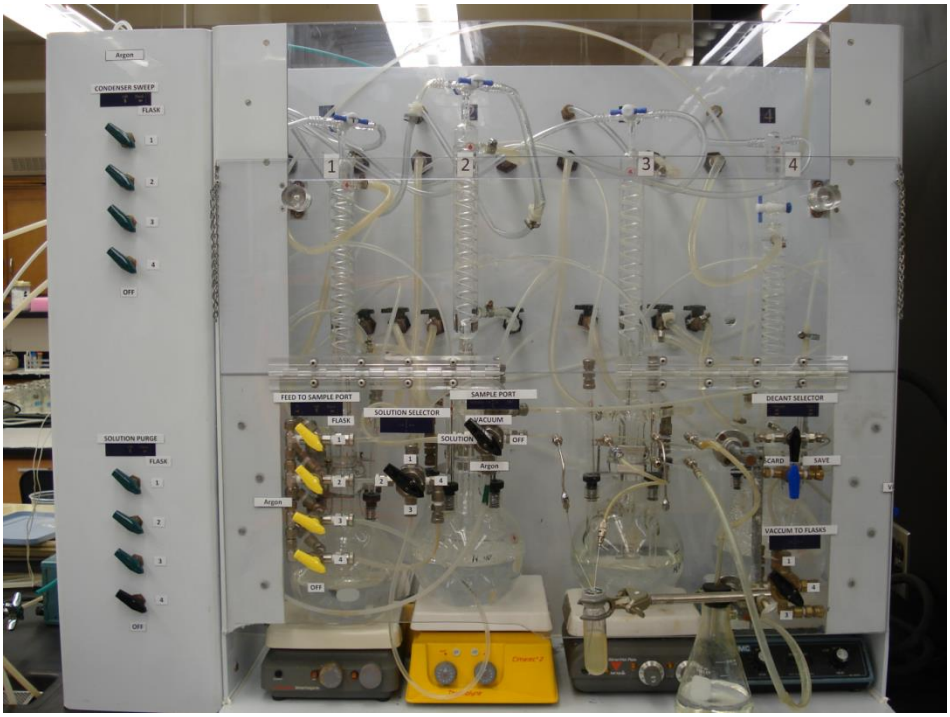

744

745

746 Figure 4

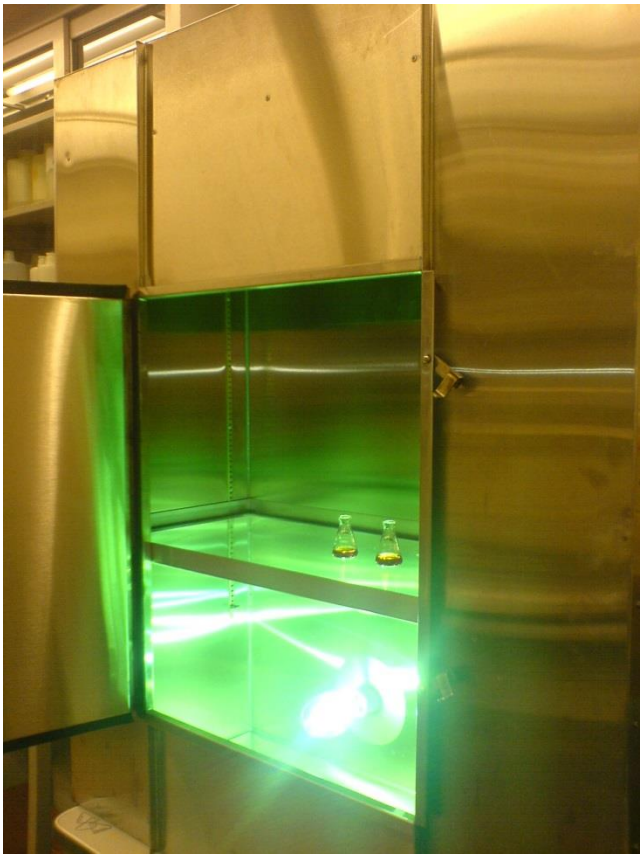

747

748

749 Figure 5

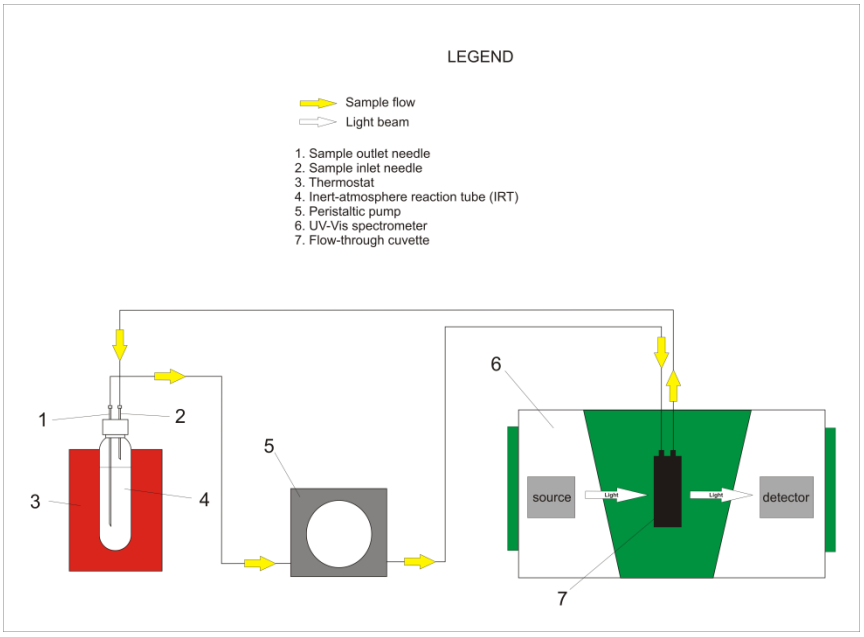

750

751

752 Figure 6

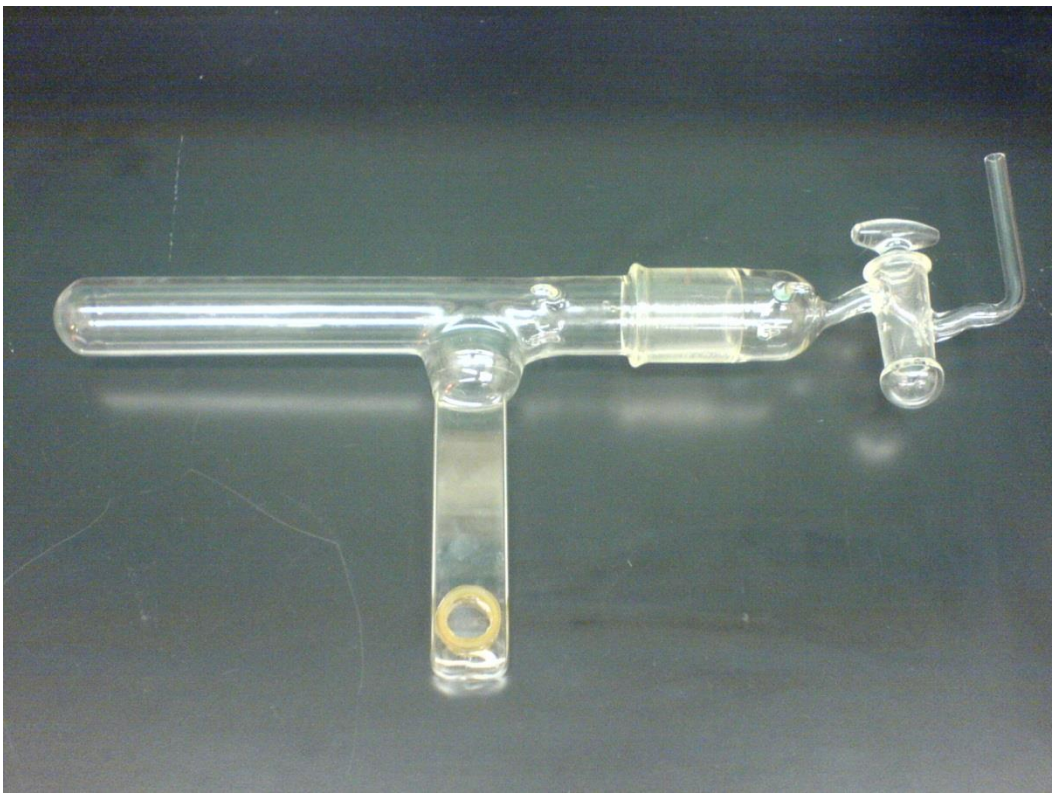

753

754

755
756